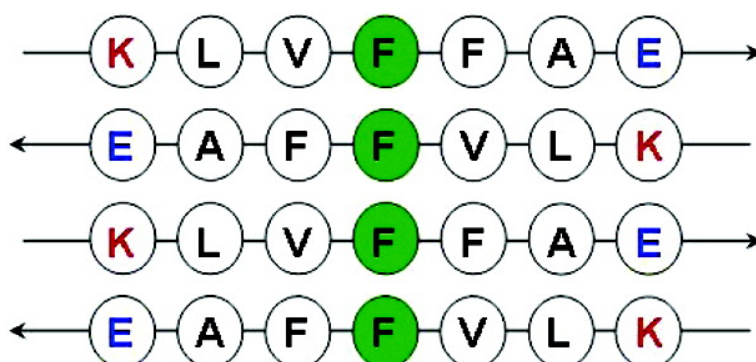


## Experimental Evidence for the Reorganization of $\beta$ -Strands within Aggregates of the A $\beta$ (16–22) Peptide

Sarah A. Petty, and Sean M. Decatur

*J. Am. Chem. Soc.*, **2005**, 127 (39), 13488-13489 • DOI: 10.1021/ja054663y • Publication Date (Web): 13 September 2005

Downloaded from <http://pubs.acs.org> on March 25, 2009



### More About This Article

Additional resources and features associated with this article are available within the HTML version:

- Supporting Information
- Links to the 11 articles that cite this article, as of the time of this article download
- Access to high resolution figures
- Links to articles and content related to this article
- Copyright permission to reproduce figures and/or text from this article

[View the Full Text HTML](#)

## Experimental Evidence for the Reorganization of $\beta$ -Strands within Aggregates of the A $\beta$ (16–22) Peptide

Sarah A. Petty and Sean M. Decatur\*

Department of Chemistry, Mount Holyoke College, South Hadley, Massachusetts 01075

Received July 13, 2005; E-mail: sdecatur@mtholyoke.edu

The misfolding of proteins and their subsequent aggregation into amyloidogenic deposits is associated with many diseases, including the Prion diseases (such as Scrapie, Bovine spongiform encephalopathy, and Creutzfeldt-Jakob disease), Type II diabetes, and Alzheimer's disease (AD).<sup>1</sup> The precise mechanism of neurotoxicity remains uncertain, although it is generally agreed that an early step in the aggregation process is the adoption of a  $\beta$ -sheet structure. Hence, the formation and stabilization of  $\beta$ -sheets is of significant importance in understanding the aggregation process.

The amyloid deposits, which accumulate in the brains of patients with AD, contain large amounts of the 40–42 residue  $\beta$ -amyloid peptides.<sup>2</sup> Several short sequences from the full-length  $\beta$ -amyloid, for example, A $\beta$ (1–28),<sup>3</sup> A $\beta$ (9–25),<sup>4</sup> A $\beta$ (10–35),<sup>5,6</sup> A $\beta$ (10–23),<sup>7</sup> A $\beta$ (16–22),<sup>8</sup> A $\beta$ (26–33),<sup>9</sup> and A $\beta$ (34–42),<sup>9,10</sup> have been shown to form amyloid fibrils in isolation. The central, hydrophobic core of this peptide, residues 16–22 (A $\beta$ (16–22)), has been studied extensively by computational chemists using molecular dynamics simulations<sup>11–13</sup> and an activation–relaxation technique (ART).<sup>14,15</sup> This seven-residue sequence, KLVFFAE, is of particular interest since four disease-causing mutations occur in this region.<sup>15</sup> This peptide is also one of the shortest reported amyloidogenic sequences and, due to its small size, is highly amenable to modeling studies. Results from solid-state NMR show that the peptide adopts a  $\beta$ -sheet structure within the fibrils and, more specifically, an antiparallel, in-register conformation has been observed.<sup>8</sup> This antiparallel arrangement of  $\beta$ -strands has been confirmed by simulations of A $\beta$ (16–22) in explicit aqueous solvent; Ma and Nussinov, in 2002, reported that the most stable conformation for an octamer of A $\beta$ (16–22) is that of two parallel  $\beta$ -sheets, each comprising four antiparallel  $\beta$ -strands.<sup>13</sup> The antiparallel in-register alignment was also found to be the lowest-energy conformation by Santini et al., in 2004, for dimers and trimers of A $\beta$ (16–22).<sup>14,15</sup> However, to date, there are no reports of the alignment and registry of A $\beta$ (16–22) in solution from data obtained experimentally, nor any detailed description of the mechanism of aggregate formation. Here, using an isotope-edited infrared (I-E IR) spectroscopic technique, we are able to describe the arrangement of  $\beta$ -strands of A $\beta$ (16–22) in aqueous solution at the molecular level, and moreover, we are able to comment on the method of rearrangement of these strands from their initial state into the final, in-register antiparallel configuration. This technique provides the first experimental evidence of the arrangement of the  $\beta$ -strands of A $\beta$ (16–22) in solution; moreover, the technique is highly applicable to other  $\beta$ -sheet-forming systems and allows the dynamics of strand rearrangements to be monitored in real time.

I-E IR spectroscopy has been used to provide site-specific structural information about peptides.<sup>16–20</sup> The introduction of <sup>13</sup>C labels into the peptide backbone (at the carbonyl C) induces a resolvable shoulder to the main amide I' band, due to the decreased vibrational frequency of the heavier oscillator limiting coupling between the <sup>12</sup>C=O modes and the <sup>13</sup>C=O mode. If two <sup>13</sup>C=O

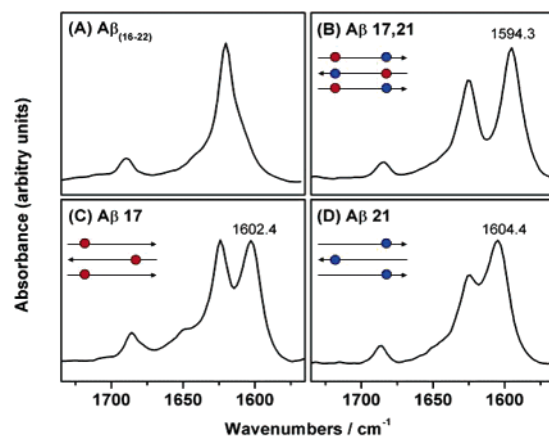


**Figure 1.** Amide I' bands of (a) unlabeled A $\beta$ (16–22) and labeled A $\beta$ (16–22) at (b) Leu17 and Ala21 simultaneously, (c) Leu17, and (d) Ala21 after heating to 75 °C and recooling to 25 °C. The frequency of the <sup>13</sup>C-labeled carbonyl vibrations are indicated. The insets indicate the  $\beta$ -strands with filled circles representing the <sup>13</sup>C-labeled residues; residue 17 is red and residue 21 is blue.

oscillators are close enough, the <sup>13</sup>C amide I' frequency is further reduced due to coupling between the <sup>13</sup>C modes. Thus, by systematic labeling of the residues of A $\beta$ (16–22), specific points of interstrand contact can be determined in the same way as has been done previously for the case of the prion peptide PrP(109–122).<sup>18,19</sup>

An unlabeled A $\beta$ (16–22) peptide was synthesized together with five variants carrying a single <sup>13</sup>C label (residues 17–21 sequentially) and a variant with residues 17 and 21 labeled simultaneously.<sup>21</sup> IR measurements were made on each sample<sup>22</sup> and on a 1:1 mixture of the unlabeled peptide and the doubly labeled peptide. The IR spectra of the unlabeled peptide and of several labeled variants are shown in Figure 1.

The spectrum of the unlabeled peptide has the distinct shape of a  $\beta$ -sheet: two narrow bands centered at around 1620 and 1690  $\text{cm}^{-1}$ . The absence of intensity around 1650  $\text{cm}^{-1}$ , which would be attributed to random coil structure, suggests in-register  $\beta$ -sheets since an “over-hang” of residues caused by a significantly out of register alignment would give rise to some random coil signal.<sup>19</sup> Irrespective of which of the residues is labeled, the introduction of a single <sup>13</sup>C carbonyl results in a narrow, resolvable band at around 1600  $\text{cm}^{-1}$ , which is assigned to  $\beta$ -sheet and indicates that all five central residues of A $\beta$ (16–22) are in the  $\beta$ -sheet conformation. Very similar frequencies for the <sup>13</sup>C band are observed if residues 17, 18, 20, or 21 are labeled individually (1601–1604  $\text{cm}^{-1}$ ; see Figure 1 and Supporting Information). However, if residue 19 is labeled individually or residues 17 and 21 are labeled simultaneously, the <sup>13</sup>C amide I' band is found, after equilibration, at approximately 1593–1594  $\text{cm}^{-1}$ . This is consistent with an antiparallel  $\beta$ -sheet model, in which the <sup>13</sup>C-labeled carbonyl of

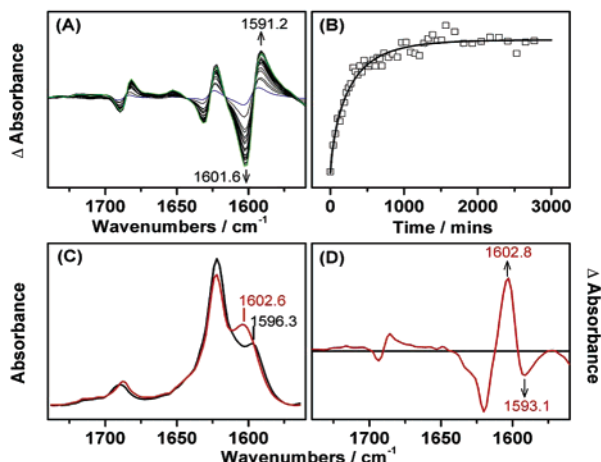


**Figure 2.** (A) Difference spectra of A $\beta$  17, 21 collected over time at 55 °C. (B) Kinetic trace for the alignment of A $\beta$  at 55 °C; the absorbance at 1591 cm<sup>-1</sup> is plotted against time. (C) The amide I band of a 1:1 mixture of unlabeled A $\beta$ (16–22) and A $\beta$  17, 21 at 25 °C before (black) and after (red) heating to 75 °C. (D) The difference spectra calculated by subtracting the initial 25 °C spectrum from the final spectrum.

residue 17 can couple with the <sup>13</sup>C-labeled carbonyl of residue 21; thus, residue 19 is in-register across all strands also resulting in coupling. These results conclusively rule out a parallel strand alignment since this would mean the ability of the <sup>13</sup>C carbonyls to couple would be equivalent for each residue, and therefore, very similar vibrational frequencies would be observed regardless of the residue labeled.

The initially formed  $\beta$ -sheets do not have this equilibrium alignment. The position of the <sup>13</sup>C band of A $\beta$  17, 21 and A $\beta$  19 moves to lower frequency as the peptide strands come into register. This realignment occurs with prolonged incubation at a given temperature or following a heat/cool cycle. Figure 2A shows the difference spectra calculated from data collected at 55 °C over 2 days; the initial spectrum was subtracted from all subsequent spectra. The increase in absorbance at 1591 cm<sup>-1</sup> is due to the labeled carbonyls aligning to enable coupling. Figure 2B shows the increase in absorbance at 1591 cm<sup>-1</sup> plotted against time and fit to a stretched exponential function. The alignment process proceeds more quickly at high temperature (see Supporting Information).

In combining samples of unlabeled A $\beta$ (16–22) and A $\beta$  17, 21, we are able to show that during this alignment process there is a mixing of strands from preformed domains of labeled and unlabeled  $\beta$ -sheets. Figure 2C shows the <sup>13</sup>C band of the mixture shifting toward higher frequency as the anneal cycle proceeds, indicating a decrease in the ability of the <sup>13</sup>C-labeled carbonyls to couple. This is further emphasized by the difference spectra in Figure 2D, which show a decreasing absorbance at 1593 cm<sup>-1</sup> and a concordant increase in intensity at 1603 cm<sup>-1</sup>.

The amide I band shows no features attributable to the random coil configuration, indicating that there is no pool of monomer in the solution since monomeric A $\beta$ (16–22) predominantly adopts a random coil configuration.<sup>15</sup> Therefore, a realignment mechanism similar to that observed at low concentration for the H1 prion peptide (PrP(109–122))<sup>23</sup> of continuous detachment of  $\beta$ -strands from the sheet and then reattachment of peptide strands from the pool of monomer onto the sheet in the correct registry is inappropriate here. Despite this, the spectral features can only be explained by a mechanism which results in the mixing of labeled and unlabeled strands; hence, we conclude that there is a rapid interchange of strands from sheets of unlabeled A $\beta$ (16–22) and

sheets of A $\beta$  17, 21. The kinetics of this process are expected to be concentration-dependent and are currently under investigation.

The process whereby peptide strands come together rapidly to form  $\beta$ -sheets and then rearrange themselves into a more favorable registry has been observed experimentally for PrP(109–122)<sup>18,19,23</sup> as well as through simulations.<sup>14,15</sup> Previous work in this group has exposed the significance of a peptide adopting its favored alignment in terms of its ability to go on to form stable amyloid fibrils.<sup>18</sup> The observation that A $\beta$ (16–22) also rearranges into a more stable registry suggests this realignment may be a more general process in the mechanisms of aggregation and as such, a better understanding of the process is essential for understanding the formation of amyloidogenic fibrils.

**Acknowledgment.** This work was supported by grants from the NSF (RUI 0415878), the National Institutes of Health (R15GM072508), and a Henry Dreyfus Teacher-Scholar Award.

**Supporting Information Available:** Spectra of other labeled A $\beta$  peptides. This material is available free of charge via the Internet at <http://pubs.acs.org>.

## References

- (1) Dobson, C. M. *Nature* **2002**, *418*, 729–730.
- (2) Selkoe, D. J. *J. Biol. Chem.* **1996**, *271*, 18295–18298.
- (3) Kirschner, D. A.; Inouye, H.; Duffy, L. K.; Sinclair, A.; Lind, M.; Selkoe, D. J. *Proc. Natl. Acad. Sci. U.S.A.* **1987**, *84*, 6953–6957.
- (4) Huang, T.; Fraser, P. E.; Chakrabarty, A. *J. Mol. Biol.* **1997**, *269*, 214–224.
- (5) Benzinger, T. L. S.; Gregory, D. M.; Burkoth, T. S.; Miller-Auer, H.; Lynn, D. G.; Botto, R. E.; Meredith, S. C. *Biochemistry* **2000**, *39*, 3491–3499.
- (6) Benzinger, T. L. S.; Gregory, D. M.; Burkoth, T. S.; Miller-Auer, H.; Lynn, D. G.; Meredith, S. C.; Botto, R. E. *Proc. Natl. Acad. Sci. U.S.A.* **1998**, *95*, 13407–13412.
- (7) Hilbich, C.; Kisters-Woike, B.; Reed, J.; Masters, C. L.; Beyreuther, K. *Eur. J. Biochem.* **1991**, *201*, 61–69.
- (8) Balbach, J. J.; Ishii, Y.; Antzutkin, O. N.; Leapman, R. D.; Rizzo, N. W.; Dyda, F.; Reed, J.; Tycko, R. *Biochemistry* **2000**, *39*, 13748–13759.
- (9) Halverson, K. J.; Fraser, P. E.; Kirschner, D. A.; Lansbury, P. T., Jr. *Biochemistry* **1990**, *29*, 2639–2644.
- (10) Lansbury, P. T., Jr.; Costa, P. R.; Griffiths, J. M.; Simon, E. J.; Auger, M.; Halverson, K. J.; Kocisko, D. A.; Hendsch, Z. S.; Ashburn, T. T.; Spencer, R. G. S.; Tidor, B.; Griffin, R. G. *Nat. Struct. Biol.* **1995**, *2*, 990–998.
- (11) Klimov, D. K.; Straub, J. E.; Thirumalai, D. *Proc. Natl. Acad. Sci. U.S.A.* **2004**, *101*, 14960–14965.
- (12) Klimov, D. K.; Thirumalai, D. *Structure* **2003**, *11*, 295–307.
- (13) Ma, B.; Nussinov, R. *Proc. Natl. Acad. Sci. U.S.A.* **2002**, *99*, 14126–14131.
- (14) Santini, S.; Mousseau, N.; Derreumaux, P. *J. Am. Chem. Soc.* **2004**, *126*, 11509–11516.
- (15) Santini, S.; Wei, G.; Mousseau, N.; Derreumaux, P. *Structure* **2004**, *12*, 1245–1255.
- (16) Decatur, S. M. *Biopolymers* **2000**, *54*, 180–185.
- (17) Decatur, S. M.; Antonic, J. *J. Am. Chem. Soc.* **1999**, *121*, 11914–11915.
- (18) Petty, S. A.; Adalsteinsson, T.; Decatur, S. M. *Biochemistry* **2005**, *44*, 4720–4726.
- (19) Silva, R. A. G. D.; Barber-Armstrong, W.; Decatur, S. M. *J. Am. Chem. Soc.* **2003**, *125*, 13674–13675.
- (20) Silva, R. A. G. D.; Nguyen, J. Y.; Decatur, S. M. *Biochemistry* **2002**, *41*, 15296–15303.
- (21) Peptides (with sequence Ac-KLVFFAE-NH<sub>2</sub>) were synthesized on a Pioneer peptide synthesizer using standard Fmoc chemical techniques. The peptides were cleaved from the resin using a trifluoroacetic acid/triisopropylsilane/water mixture, purified by reverse-phase HPLC, characterized by electrospray mass spectrometry, and exchanged in 0.05 mM DCl for 6–8 h.
- (22) For IR samples, 1–2 mg of peptide was dissolved in 100  $\mu$ L of deuterated phosphate buffer (1 mM potassium phosphate) at pH 7. The samples were loaded into an IR cell fitted with calcium fluoride windows and separated by a 100  $\mu$ m Teflon spacer. The sample was temperature-controlled externally by a water bath. IR measurements were taken on a Vector 22 FTIR spectrometer (Bruker) operating at a resolution of 4 cm<sup>-1</sup> and averaging over 512 scans. Spectra were collected at 25–75 °C in 10° intervals. The sample temperature was maintained at 75 °C for 3 h before re-equilibrating at 25 °C and recording a final IR spectrum.
- (23) Petty, S. A.; Decatur, S. M. Kinetics of  $\beta$ -Sheet Alignment and Fiber Formation in the Prion Peptide. National Meeting of the American Chemical Society, San Diego, 2005.

JA054663Y